Signal Processing 227 (2025) 109709

Contents lists available at ScienceDirect

Signal Processing

journal homepage: www.elsevier.com/locate/sigpro

Short communication

Sparse channel estimation for underwater acoustic OFDM systems with super-nested pilot design

Lei Wan [a,b], Shuimei Deng [a,b], Yougan Chen [a,c,*], En Cheng [a,b]

[a] Key Laboratory of Underwater Acoustic Communication and Marine Information Technology (Xiamen University), Ministry of Education, Xiamen, 361005, China
[b] School of Informatics, Xiamen University, Xiamen, 361005, China
[c] College of Ocean and Earth Sciences, Xiamen University, Xiamen, 361102, China

ARTICLE INFO

Keywords:
Sparse channel estimation
Underwater acoustic OFDM
Super-nested array
Virtual pilot
Covariance matrix refinement

ABSTRACT

Underwater acoustic channels are usually sparse and have large delay spread. In this paper, super-nested array structure in the field of array signal processing is borrowed to be the pilot design of underwater acoustic OFDM systems, in order to better estimate large delay spread channels with limited number of pilots. Specifically, by constructing the pilot subcarriers' covariance matrix and the pilot position difference, the virtual pilot on the differential co-array are employed for sparse channel estimation. In order to reduce the error between the estimated pilot subcarriers' covariance matrix and the ideal covariance matrix, the cross-correlation matrix of pilot subcarriers is estimated in advance for interference cancellation. Then the sparse iterative covariance estimation algorithm (SPICE) is adopted to further refine the covariance matrix and improve the channel estimation performance. Simulation, pool and sea experimental results show that the proposed method can effectively estimate the large delay spread sparse channels and improve the performance of underwater acoustic OFDM systems.

1. Introduction

Due to the slow transmission speed of underwater acoustic waves, reflections from the bottom and surface, as well as refraction of underwater acoustic waves lead the signal reach the receiver in different directions and paths, resulting in significant multipath delay spread of the underwater acoustic communication channels [1]. Orthogonal frequency division multiplexing (OFDM) technology has the advantages of low complexity equalization of multipath channel and high bandwidth efficiency, hence it has been widely used in underwater acoustic communication systems [2–4]. In terms of channel estimation, the simple least squares (LS) and subspace multiple signal classification (MUSIC) algorithm have been applied to underwater acoustic OFDM systems. Taking advantage of the sparsity of underwater acoustic channels, compressed sensing technology was proposed and it is still very popular nowadays [5]. Among the compressed sensing techniques, orthogonal matching pursuit (OMP) has relatively lower computational complexity [6], and therefore it is widely adopted [5,7,8].

For coherent communication systems, pilots are needed for accurate channel estimation. A significant amount of underwater acoustic OFDM systems adopt uniform pilot distribution for channel estimation [5,8]. However, due to the existence of periodicity, uniform pilot distribution faces the problem of limited estimation range. For example, in an OFDM system with a symbol duration of T and a uniform pilot interval of D, only the delay within T/D can be effectively estimated. In order to estimate the delay beyond the range, it is necessary to further reduce the pilot interval and increase the number of pilots, which means that valuable bandwidth resources are wasted. On the other hand, if random pilot distribution is used for channel estimation of OFDM systems, the accuracy of channel estimation generally deteriorates [9]. In order to solve this problem, according to the equivalence between path delay estimation in OFDM systems and direction of arrival (DOA) estimation in antenna array processing [10], this paper refers to array element distribution for the pilot design of underwater acoustic OFDM systems.

According to the classical coprime array theory [11], in order to improve the direction finding ability, the design schemes such as coprime array with compressed inter-element spacing (CACIS), coprime array with displaced subarrays (CADiS) based on the ion array and multi-order super-nested array have been widely used [12,13]. These array structures have a common feature, that is, the spacing between the array elements is not uniform and the difference co-matrix is constructed from the array element covariance matrix. In the difference domain, the increase of the continuous position difference means the increase of the number of virtual array elements, which further increases the degree of freedom and improves the estimation accuracy. As a result,

* Correspondence to: Rm. C3-216, Xiping Bldg., Xiang'an Campus of Xiamen University, Xiamen, 361102, China.
E-mail address: chenyougan@xmu.edu.cn (Y. Chen).

https://doi.org/10.1016/j.sigpro.2024.109709
Received 1 October 2023; Received in revised form 3 September 2024; Accepted 9 September 2024
Available online 12 September 2024

Table 1
Symbols used in this paper.

N	Number of subcarriers	T	Symbol duration
T_{cp}	Cyclic-prefix length	B	Bandwidth
f_c	Carrier frequency	N_p	Number of pilots
$s[k]$	Data symbol on the kth subcarrier	$\widetilde{x}(t)$	Passband OFDM symbol
$q(t)$	Rectangular pulse shaping window	L	Multipath number
$h(t)$	Channel impulse response	$\delta(t)$	Dirac delta function
A_l	Amplitude of lth path	τ_l	Delay of lth path
$z[k]$	Observation on the kth subcarrier	$w[k]$	Noise on the kth subcarrier
$\mathbb{P}$	Set of pilot subcarrier indices	$\check{\boldsymbol{z}}$	Pilot subcarrier observation vector after compensation
$\boldsymbol{a}_{\tau_1}$	Steering vector of the lth path	$\boldsymbol{A}$	Matrix consisting of all $\boldsymbol{a}_{\tau_1}$
$\boldsymbol{P}_m$	Position of the mth pilot	ξ_l	Equivalent amplitude of the lth multipath
$\boldsymbol{\xi}$	Vector consisting of all ξ_l	$\boldsymbol{n}$	Equivalent noise vector after compensation
δ_n^2	Noise power	$\boldsymbol{R}_{zz}$	Ideal pilot subcarrier covariance matrix
$\boldsymbol{R}_s$	Diagonal matrix consisting of ξ_l^2	N_1	Number of snapshots of the received signal
$\boldsymbol{I}_{N_p}$	$N_p \times N_p$ unit matrix	$\boldsymbol{M}_1$ & $\boldsymbol{M}_2$	Number of pilots in the two sub-arrays
$\mathbb{C}_p$	Set of pilot position difference	$\boldsymbol{R}_{cor}$	Cross-correlation interference between paths
$\hat{(\cdot)}$	Estimated value of $(\cdot)$	$\bar{\boldsymbol{R}}_{zz}^1$	Pilot subcarrier covariance matrix (limited snapshots)
λ	Oversampling factor in delay estimation	Q	Number of candidates in dictionary matrix
τ_{max}	Maximum path delay	$\tilde{\boldsymbol{A}}$	Constructed dictionary matrix
$\tilde{\boldsymbol{\xi}}$	Equivalent path amplitude vector	$\tilde{\boldsymbol{n}}$	Equivalent noise vector in delay estimation
$\bar{\boldsymbol{A}}, \bar{\boldsymbol{R}}_s, \boldsymbol{B}$	Steering vector, power, and equivalent power matrices in delay estimation with enough snapshots		
$\boldsymbol{R}_{zz}^{-1/2}$	Positive definite square-root of $\boldsymbol{R}_{zz}^{-1}$	p_k	Equivalent power of the kth multipath delay: ξ_k^2
$\boldsymbol{r}$, $\tilde{\boldsymbol{I}}$	Matrices $\boldsymbol{R}_{zz}$,$\boldsymbol{I}_{N_p}$ vectorized	$\boldsymbol{b}$	Equivalent path power vector: $[\xi_1^2, \xi_2^2, ..., \xi_Q^2]^T$
$\bigotimes$	Kronecker product	$\tilde{\boldsymbol{A}}$	$[\tilde{\boldsymbol{a}}_1, \tilde{\boldsymbol{a}}_2, ..., \tilde{\boldsymbol{a}}_Q]$, each column $\tilde{\boldsymbol{a}}_i = \boldsymbol{a}_i^* \bigotimes \boldsymbol{a}_i$
$\boldsymbol{r}_1$, $\tilde{\boldsymbol{A}}_1$, $\tilde{\boldsymbol{I}}_1$:	Constructed from $\boldsymbol{r}$, $\tilde{\boldsymbol{A}}$, $\tilde{\boldsymbol{I}}$, with elements, rows corresponding to virtual pilots selected		
$\boldsymbol{J}_m$	Position index of the virtual pilots	N_c	Symbol number for time-varying channel estimation
$\boldsymbol{\alpha}_l$	Complex gain of the lth path	T_s	Sample interval
N_g	Sample length of CP	v	Total sample length of OFDM symbol: $N + N_g$
$\tilde{\boldsymbol{\alpha}}_l$	Average complex gain of the lth path	$\boldsymbol{c}_l$	Vector of N_c polynomial coefficients for the lth path
$\boldsymbol{c}_{des_l}$	Optimal solution of $\boldsymbol{c}_l$	$\boldsymbol{T}$	Transformation matrix
f_d	Residual Doppler frequency shift	$\mathbb{C}$	Set of complex numbers

the DOA estimation performance of the subspace based and compressed sensing based methods can be further improved [14].

In this paper, a super-nested pilot distribution is designed for underwater acoustic OFDM systems to improve the performance of channel estimation in large delay spread channels. By constructing the pilot covariance matrix and the pilot position difference, the pilot covariance matrix elements corresponding to the continuous position difference are obtained and rearranged on the basis of the differential co-array. Then, they are used as the continuous uniform virtual pilot, based on which the channel is estimated through compressed sensing algorithms such as OMP.

The contributions of this paper include:

1. A pilot design of super-nested structure is proposed for underwater acoustic OFDM systems in sparse channels with large delay spread.
2. Estimation of cross correlation between pilot subcarriers and sparse iterative covariance estimation (SPICE) algorithm are adopted to process the covariance matrix for better estimation performance.
3. Simulation, pool and sea experimental results are utilized to verify the effectiveness of the proposed scheme.

The paper is organized as follows. The system model and the pilot design are given in Section 2. The sparse channel estimation scheme is described in Section 3. The simulation and experimental results are provided in Section 4 and Section 5, respectively. The concluding remarks are given in Section 6. Table 1 lists out the important mathematical symbols used in this paper, most of which will be introduced in more details when they are defined.

2. System model

2.1. OFDM system model

In this paper, cyclic prefix (CP) OFDM is considered. Assume one OFDM symbol consists of N subcarriers. The OFDM symbol duration is T, the length of the cyclic prefix is T_{cp}, the subcarrier spacing is $1/T$, and the system bandwidth $B = N/T$. The kth subcarrier is at frequency

$$f_k = f_c + \frac{k}{T},\ k = -\frac{N}{2}, \dots, \frac{N}{2} - 1 \tag{1}$$

where the carrier frequency is f_c. Denote the data symbol transmitted on the kth subcarrier to be $s[k]$, the passband OFDM symbol to be transmitted can be expressed as

$$\widetilde{x}(t) = 2\mathrm{Re}\left\{ \sum_{k=-N/2}^{N/2-1} s[k] e^{j2\pi f_k t} q(t) \right\} \tag{2}$$

where $q(t)$ is the rectangular pulse shaping window,

$$q(t) = \begin{cases} 1, & t \in [-T_{cp}, T] \\ 0, & \text{elsewhere} \end{cases} \tag{3}$$

The adopted channel model is a multipath channel with L paths, the amplitude and delay of each path are A_l and τ_l ($l = 1, 2, \dots, L$), respectively. Since there have been many related work on wideband Doppler estimation and compensation for underwater acoustic OFDM systems, we focus on the cases of no Doppler effect or only residual narrow band Doppler effect in this paper. In case without Doppler, the channel impulse response $h(t)$ can be written as

$$h(t) = \sum_{l=1}^{L} A_l \delta(t - \tau_l) \tag{4}$$

At the receiver, after downshifting, low-pass filtering, CP removal (assume it is longer than the maximum delay spread), and fast Fourier transform (FFT) demodulation, the data on the kth subcarrier can be expressed as

$$z[k] = \sum_{l=1}^{L} A_l s[k] e^{-j2\pi f_k \tau_l} + w[k] \tag{5}$$

where $w[k]$ is the additive noise. Among N subcarriers, it is assumed that there are N_p pilot subcarriers, which are used for channel estimation. Furthermore, the set of pilot subcarrier indices is denoted as $\mathbb{P}$.

After compensating the received frequency domain observation vector by pilots, the input–output relationship on the pilot subcarriers can be expressed as

$$\check{\boldsymbol{z}} = \boldsymbol{A}\boldsymbol{\xi} + \boldsymbol{n} \tag{6}$$

where $\check{\boldsymbol{z}}, \boldsymbol{n} \in \mathbb{C}^{N_p \times 1}$ represent the equivalent received observation vector and the equivalent noise vector, respectively. $\boldsymbol{A} = [\boldsymbol{a}_{\tau_1}, \boldsymbol{a}_{\tau_2}, \dots, \boldsymbol{a}_{\tau_L}]$, the lth column vector $\boldsymbol{a}_{\tau_l}$ in $\boldsymbol{A}$ corresponds to the contribution of the lth multipath. $\boldsymbol{a}_{\tau_l}[m] = e^{-j2\pi(f_c + P_m/T)\tau_l}$ $(m = 0, 1, \dots, N_p - 1)$, P_m is the position of the mth pilot, $P_m \in \mathbb{P}$. $\boldsymbol{\xi} = [\xi_1, \xi_2, \dots, \xi_L]^T$ is the equivalent amplitude vector of each multipath component, where $(\cdot)^T$ denotes the transpose of $(\cdot)$.

It is assumed that the signals of each path are independent of each other. When the number of snapshots of the received signal N_1 is large enough, the pilot subcarrier covariance matrix can be expressed as

$$\boldsymbol{R}_{zz} = E[\check{\boldsymbol{z}}\check{\boldsymbol{z}}^H] = \frac{1}{N_1}\sum_{n=1}^{N_1}\check{\boldsymbol{z}}_n\check{\boldsymbol{z}}_n^H = \boldsymbol{A}\boldsymbol{R}_s\boldsymbol{A}^H + \delta_n^2\boldsymbol{I}_{N_p} = \sum_{l=1}^{L}\xi_l^2\boldsymbol{a}_{\tau_l}\boldsymbol{a}_{\tau_l}^H + \delta_n^2\boldsymbol{I}_{N_p} \tag{7}$$

where $(*)^H$ denotes the conjugate transpose operator, $\check{\boldsymbol{z}}_n$ denotes the nth pilot-compensated received signal, $\boldsymbol{R}_s = diag(\xi_1^2, \xi_2^2, \dots, \xi_L^2)$, ξ_l^2 represents the power of the lth multipath, δ_n^2 is the noise power, and $\boldsymbol{I}_{N_p}$ is the $N_p \times N_p$ unit matrix.

2.2. Pilot design

The pilot distribution of OFDM is designed as a super-nested array structure to obtain the maximum number of continuous pilot position difference. The super-nested array can be subdivided into first-order, second-order, third-order and more. In this paper, taking the second-order super-nested array structure as an example, we assume that the number of pilots in the two sub-arrays is M_1 and M_2, respectively, where $M_1 \geq 4$, $M_2 \geq 3$. Then the pilot position set $\mathbb{P}$ satisfies the following relationship

$$\mathbb{P} = \mathbb{X}_1 \cup \mathbb{Y}_1 \cup \mathbb{X}_2 \cup \mathbb{Y}_2 \cup \mathbb{Z}_1 \cup \mathbb{Z}_2 \tag{8}$$

where,

$$\begin{aligned}
&\mathbb{X}_1 = \{1 + 2q \mid 0 \leq q \leq A_1\} \\
&\mathbb{Y}_1 = \{(M_1 + 1) - (1 + 2q) \mid 0 \leq q \leq B_1\} \\
&\mathbb{X}_2 = \{(M_1 + 1) + (2 + 2q) \mid 0 \leq q \leq A_2\} \\
&\mathbb{Y}_2 = \{2(M_1 + 1) - (2 + 2q) \mid 0 \leq q \leq B_2\} \\
&\mathbb{Z}_1 = \{q(M_1 + 1) \mid 2 \leq q \leq M_2\} \\
&\mathbb{Z}_2 = \{M_2(M_1 + 1) - 1\}
\end{aligned} \tag{9}$$

The parameters A_1, B_1, A_2, B_2 are defined by the following

$$(A_1, B_1, A_2, B_2) = \begin{cases} (r, r-1, r-1, r-2), & M_1 = 4r \\ (r, r-1, r-1, r-1), & M_1 = 4r+1 \\ (r+1, r-1, r, r-2), & M_1 = 4r+2 \\ (r, r, r, r-1), & M_1 = 4r+3 \end{cases} \tag{10}$$

where r is an integer.

The (i, j)th element of the pilot subcarriers covariance matrix $\boldsymbol{R}_{zz}$ comes from the contribution of all paths $\boldsymbol{a}_{\tau_l}[i]\boldsymbol{a}_{\tau_l}[j]^H$. For all l, the value $\boldsymbol{a}_{\tau_l}[i]\boldsymbol{a}_{\tau_l}[j]^H$ is depended on the difference between the positions of the ith and the jth pilots. Using the above super-nested structure pilot distribution, the set of pilot position difference is given by

$$\mathbb{C}_p = \{k | k = u - v, u \in \mathbb{P}, v \in \mathbb{P}\} \tag{11}$$

Obviously, there are many repeated elements in $\mathbb{C}_p$, indicating that the covariance matrix $\boldsymbol{R}_{zz}$ has many repeated elements. For channel estimation, the longest continuous position difference is selected from the pilot position difference set $\mathbb{C}_p$, and the corresponding elements are obtained from the covariance matrix $\boldsymbol{R}_{zz}$ to form the virtual pilots.

Based on the obtained virtual pilots, compressed sensing algorithms such as OMP can be utilized to estimate the multipath delays and amplitudes. However, in practical communication systems, the number of snapshots of received signal is usually limited, and hence the ideal covariance matrix $\boldsymbol{R}_{zz}$ shown in Eq. (7) is not available. In the next section, methods will be introduced to overcome this issue.

3. The proposed channel estimation scheme

3.1. Initial cross-correlation interference estimation

When the number of snapshots of the received signal $\check{\boldsymbol{z}}$ is small (taking 1 as an example), the cross-correlation interference $\boldsymbol{R}_{cor}$ between each path's signal should be considered. Then pilot subcarrier covariance matrix model is modified to

$$\begin{aligned}
\bar{\boldsymbol{R}}_{zz}^1 &= \check{\boldsymbol{z}}\check{\boldsymbol{z}}^H \\
&= \boldsymbol{A}\boldsymbol{R}_s\boldsymbol{A}^H + \delta_n^2\boldsymbol{I}_{N_p} + \boldsymbol{R}_{cor} \\
&= \sum_{l=1}^{L}\xi_l^2\boldsymbol{a}_{\tau_l}\boldsymbol{a}_{\tau_l}^H + \delta_n^2\boldsymbol{I}_{N_p} + \sum_{i=1}^{L}\sum_{j=1, i\neq j}^{L}\xi_i\xi_j\boldsymbol{a}_{\tau_i}\boldsymbol{a}_{\tau_j}^H
\end{aligned} \tag{12}$$

In this paper, we propose to carry out an initial channel estimation for the reconstruction of $\boldsymbol{R}_{cor}$. The pilot-compensated signal $\check{\boldsymbol{z}}$ is adopted to estimated the multipath delay $\hat{\tau}_l$ and amplitude $\hat{\xi}_l$ directly. Then the steering vector $\hat{\boldsymbol{a}}_{\hat{\tau}_l} = \left[e^{-j2\pi(f_c + P_0/T)\hat{\tau}_l}, e^{-j2\pi(f_c + P_1/T)\hat{\tau}_l}, \dots, e^{-j2\pi(f_c + P_{N_p-1}/T)\hat{\tau}_l}\right]^T$ from the multipath delay $\hat{\tau}_l$ is established, and an estimate of the cross-correlation $\hat{\boldsymbol{R}}_{cor}$ can be obtained

$$\hat{\boldsymbol{R}}_{cor} = \sum_{i=1}^{\hat{L}}\sum_{j=1, i\neq j}^{\hat{L}}\hat{\xi}_i\hat{\xi}_j\hat{\boldsymbol{a}}_{\hat{\tau}_i}\hat{\boldsymbol{a}}_{\hat{\tau}_j}^H \tag{13}$$

where $\hat{L}$ is the number of estimated multipath.

Using $\hat{\boldsymbol{R}}_{cor}$ for interference cancellation, the estimated pilot subcarrier covariance matrix can be expressed as

$$\hat{\boldsymbol{R}}_{zz}^1 = \bar{\boldsymbol{R}}_{zz}^1 - \hat{\boldsymbol{R}}_{cor} = \check{\boldsymbol{z}}\check{\boldsymbol{z}}^H - \hat{\boldsymbol{R}}_{cor} \tag{14}$$

It is worth mentioning that the initial channel estimation for interference reconstruction based on $\check{\boldsymbol{z}}$ can be carried out through several algorithms, such OMP based compressed sensing method.

3.2. Further covariance matrix refinement

In order to further reduce the error between the estimated pilot subcarrier covariance matrix and the ideal pilot subcarrier covariance matrix, SPICE algorithm is applied to estimated the pilot subcarrier covariance matrix. By constructing a dictionary matrix, we sparsely represent the received signal on the pilot subcarrier in (6). Define $Q = [\lambda B \cdot \tau_{max}] + 1$, where λ and τ_{max} are the oversampling factor and the maximum delay, respectively. Thus, the equivalent channel input–output relationship in matrix vector form can be expressed as

$$\check{\boldsymbol{z}} = \bar{\boldsymbol{A}}\bar{\boldsymbol{\xi}} + \bar{\boldsymbol{n}} \tag{15}$$

where $\bar{\boldsymbol{A}} \in \mathbb{C}^{N_p \times Q}$, $\bar{\boldsymbol{\xi}} \in \mathbb{C}^{Q \times 1}$ and $\bar{\boldsymbol{n}} \in \mathbb{C}^{N_p \times 1}$ are the dictionary matrix, the equivalent path amplitude vector and the equivalent noise vector, respectively. $\bar{\boldsymbol{A}}$ and $\bar{\boldsymbol{\xi}}$ are defined as

$$\begin{aligned}
&\bar{\boldsymbol{A}} = [\boldsymbol{a}_1, \dots, \boldsymbol{a}_i, \dots, \boldsymbol{a}_Q] \\
&\bar{\boldsymbol{\xi}} = [\xi_1, \dots, \xi_i, \dots, \xi_Q]^T
\end{aligned} \tag{16}$$

where the mth element of the atom $\boldsymbol{a}_i$ is $e^{-j2\pi(f_c + \frac{P_m}{T})\tau_i}$, $P_m \in \mathbb{P}$, and $\tau_i = \frac{i}{\lambda B}$.

In case the number of snapshots N_1 is large enough, the pilot subcarrier covariance matrix model in Eq. (7) can be expressed as:

$$\begin{aligned}\boldsymbol{R}_{zz} &= E[\check{\boldsymbol{z}}\check{\boldsymbol{z}}^H] = \frac{1}{N_1}\sum_{n=1}^{N_1}\check{\boldsymbol{z}}_n\check{\boldsymbol{z}}_n^H = \bar{\boldsymbol{A}}\bar{\boldsymbol{R}}_s\bar{\boldsymbol{A}}^H + \delta_n^2\boldsymbol{I}_{N_p} \\ &= \sum_{k=1}^{Q}\xi_k^2\boldsymbol{a}_k\boldsymbol{a}_k^H + \delta_n^2\boldsymbol{I}_{N_p} \triangleq \bar{\bar{\boldsymbol{A}}}\boldsymbol{B}\bar{\bar{\boldsymbol{A}}}^H\end{aligned} \tag{17}$$

where

$$\begin{aligned}&\bar{\boldsymbol{R}}_s = diag(\xi_1^2, \xi_2^2, \ldots, \xi_Q^2) \\ &\bar{\bar{\boldsymbol{A}}} \triangleq [\bar{\boldsymbol{A}} \quad \boldsymbol{I}_{N_p}] \triangleq [\boldsymbol{a}_1, \ldots, \boldsymbol{a}_Q, \boldsymbol{a}_{Q+1}, \ldots, \boldsymbol{a}_{Q+N_p}] \\ &\boldsymbol{B} \triangleq diag(\xi_1^2, \xi_2^2, \ldots, \xi_Q^2, \delta_1, \ldots, \delta_{N_p}) \triangleq diag(p_1, p_2, \ldots, p_Q, p_{Q+1}, \ldots, p_{Q+N_p})\end{aligned} \tag{18}$$

Here $\bar{\bar{\boldsymbol{A}}} \in \mathbb{C}^{N_p\times(Q+N_p)}$ and $\boldsymbol{B} \in \mathbb{C}^{(Q+N_p)\times(Q+N_p)}$ are steering vector matrix and equivalent power matrix, respectively. $p_k = \xi_k^2$ $(k = 1, 2, \ldots, Q+N_p)$ is the equivalent power corresponding to kth multipath delay.

In practical systems where the number of received signal snapshots N_1 is small, SPICE algorithm based on covariance fitting criterion is carried out, which minimizes the following f (see, e.g., [15])

$$f = \|\boldsymbol{R}_{zz}^{-1/2}(\hat{\boldsymbol{R}}_{zz} - \boldsymbol{R}_{zz})\hat{\boldsymbol{R}}_{zz}^{-1/2}\|^2 \tag{19}$$

Here, $\boldsymbol{R}_{zz}$ is the ideal covariance matrix shown in (17), $\hat{\boldsymbol{R}}_{zz}$ is the estimated covariance matrix, $\boldsymbol{R}_{zz}^{-1/2}$ denotes the positive definite square-root of $\boldsymbol{R}_{zz}^{-1}$.

Actually, minimizing the fitting criterion f is equivalent to minimize the following function

$$g = tr(\hat{\boldsymbol{R}}_{zz}^{1/2}\boldsymbol{R}_{zz}^{-1}\hat{\boldsymbol{R}}_{zz}^{1/2}) + \sum_{k=1}^{Q+N_p}(\boldsymbol{a}_k^H\hat{\boldsymbol{R}}_{zz}^{-1}\boldsymbol{a}_k)p_k \tag{20}$$

which can be reformulated as the following constrained minimization problem

$$\min_{p_k\geq 0} tr(\hat{\boldsymbol{R}}_{zz}^{1/2}\boldsymbol{R}_{zz}^{-1}\hat{\boldsymbol{R}}_{zz}^{1/2}) \quad s.t. \sum_{k=1}^{Q+N_p}\omega_k p_k = 1 \tag{21}$$

where $\omega_k = \boldsymbol{a}_k^H\hat{\boldsymbol{R}}_{zz}^{-1}\boldsymbol{a}_k/N_p$.

In summary, the problem of minimizing the fitting criterion f is transformed into an optimization problem with the equivalent power $p_k(k = 1, 2, \ldots, Q+N_p)$ constraint. In the process of fitting iteration, the algorithm first initializes the estimated covariance matrix $\hat{\boldsymbol{R}}_{zz}$ and the equivalent power p_k, then updates the current equivalent power p_k by the previous round of equivalent power. At the same time, the equivalent power matrix $\boldsymbol{B}$ is also updated. Each time the updated $\boldsymbol{B}$ is used to update the estimated covariance matrix $\hat{\boldsymbol{R}}_{zz}$ until $\hat{\boldsymbol{R}}_{zz}$ approaches the ideal covariance matrix $\boldsymbol{R}_{zz}$. The detailed process of SPICE can be seen in Algorithm 1. The variation between the current estimated covariance matrix and the one in the previous iteration, along with the maximum number of iterations are adopted as the stopping criteria for SPICE algorithm in this paper.

Algorithm 1 SPICE

Input: $\bar{\boldsymbol{R}}_{zz}$: the pilot subcarrier covariance matrix, $\hat{\boldsymbol{R}}_{cor}$: the cross-correlation interference matrix

Output: $\hat{\boldsymbol{R}}_{zz}$: estimation of covariance matrix on pilot subcarriers

Step 1: Calculate the initial covariance matrix $\hat{\boldsymbol{R}}_{zz}^1 = \bar{\boldsymbol{R}}_{zz} - \hat{\boldsymbol{R}}_{cor}$

Step 2: Initialization:

The steering vector matrix $\bar{\bar{\boldsymbol{A}}} \in \mathbb{C}^{N_p\times(Q+N_p)}$ and equivalent power matrix $\boldsymbol{B}^{ini} \in \mathbb{C}^{(Q+N_p)\times(Q+N_p)}$. The (k,k)th element of $\boldsymbol{B}^{ini}$ is $p_k^{ini} = \frac{\boldsymbol{a}_k^H\hat{\boldsymbol{R}}_{zz}^1\boldsymbol{a}_k}{\|\boldsymbol{a}_k\|^4}$. The maximum number of iterations is G, and the threshold is ε.

Calculate the initialized value:

$\boldsymbol{R}^{ini} = \bar{\bar{\boldsymbol{A}}}\boldsymbol{B}^{ini}\bar{\bar{\boldsymbol{A}}}^H$

$\omega_k = \boldsymbol{a}_k^H(\hat{\boldsymbol{R}}_{zz}^1)^{-1}\boldsymbol{a}_k/N_p$

$\rho^{ini} = \sum_{k=1}^{Q+N_p}\omega_k^{1/2}p_k^{ini}||\boldsymbol{a}_k(\boldsymbol{R}^{ini})^{-1}(\hat{\boldsymbol{R}}_{zz}^1)^{1/2}||$

$p_k^0 = p_k^{ini}\frac{||\boldsymbol{a}_k^H(\boldsymbol{R}^{ini})^{-1}(\hat{\boldsymbol{R}}_{zz}^1)^{1/2}||}{\omega_k^{1/2}\rho^{ini}}$

$\boldsymbol{B}^0 = diag\{p_1^0, p_2^0, ..., p_{Q+N_p}^0\}$

$\hat{\boldsymbol{R}}_{zz}^0 = \bar{\bar{\boldsymbol{A}}}\boldsymbol{B}^0\bar{\bar{\boldsymbol{A}}}^H$

$g = 1$

Step 3:

while $g \leq G$ & $||\hat{\boldsymbol{R}}_{zz}^g - \hat{\boldsymbol{R}}_{zz}^{g-1}|| > \varepsilon$ **do**

$\rho^{g-1} = \sum_{k=1}^{Q+N_p}\omega_k^{1/2}p_k^{g-1}||\boldsymbol{a}_k(\hat{\boldsymbol{R}}_{zz}^{g-1})^{-1}(\hat{\boldsymbol{R}}_{zz}^1)^{1/2}||$

for $k = 1 : (Q+N_p)$ **do**

$p_k^g = p_k^{g-1}\frac{||\boldsymbol{a}_k^H(\hat{\boldsymbol{R}}_{zz}^{g-1})^{-1}(\hat{\boldsymbol{R}}_{zz}^1)^{1/2}||}{\omega_k^{1/2}\rho^{g-1}}$

end for

$\boldsymbol{B}^g = diag\{p_1^g, p_2^g, ..., p_{Q+N_p}^g\}$

$\hat{\boldsymbol{R}}_{zz}^g = \bar{\bar{\boldsymbol{A}}}\boldsymbol{B}^g\bar{\bar{\boldsymbol{A}}}^H$

$g = g + 1$

end while

3.3. OMP channel estimation formulation

Assuming that we obtain the ideal pilot subcarrier covariance matrix $\boldsymbol{R}_{zz}$ after the above two steps, vectorize $\boldsymbol{R}_{zz}$ and we have

$$\boldsymbol{r} = vec(\boldsymbol{R}_{zz}) = \tilde{\boldsymbol{A}}\boldsymbol{b} + \delta_n^2\tilde{\boldsymbol{I}} \tag{22}$$

where $vec(\boldsymbol{R}_{zz})$ means that the columns of the covariance matrix $\boldsymbol{R}_{zz}$ are accumulated to form a vector, $\tilde{\boldsymbol{I}} = vec(\boldsymbol{I}_{N_p})$. $\tilde{\boldsymbol{A}} = [\tilde{\boldsymbol{a}}_1, \tilde{\boldsymbol{a}}_2, \ldots, \tilde{\boldsymbol{a}}_Q]$ where each of these columns $\tilde{\boldsymbol{a}}_i = \boldsymbol{a}_i^* \bigotimes \boldsymbol{a}_i$, $\boldsymbol{a}_i^*$ denotes the conjugate of $\boldsymbol{a}_i$, $\bigotimes$ is Kronecker product, $\boldsymbol{b} = [\xi_1^2, \xi_2^2, \ldots, \xi_Q^2]^T$ is the equivalent path power vector.

Using the super-nested structure pilot distribution, the longest continuous position difference is selected from the pilot position difference set $\mathbb{C}_p$. According to the rule of Kronecker product, the differential array of the super-nested structure is a uniform linear array with the number of $2M_1M_2 + 2M_2 - 1$ $(M_1 \geq M_2)$ elements, which is the maximum length of the continuous position difference. Specifically, the vector $\boldsymbol{r}$ is screened and rearranged in the order of pilot position difference from $-M_1M_2 - M_2 + 1$ to $M_1M_2 + M_2 - 1$, and then the received signal $\boldsymbol{r}_1$ corresponding to the virtual pilots with continuous position difference is obtained, which has the following relationship

$$\boldsymbol{r}_1 = \tilde{\boldsymbol{A}}_1\boldsymbol{b} + \delta_n^2\tilde{\boldsymbol{I}}_1 \tag{23}$$

where $\tilde{\boldsymbol{A}}_1 \in \mathbb{C}^{(2M_1M_2+2M_2-1)\times Q}$ and $\tilde{\boldsymbol{I}}_1 \in \mathbb{C}^{(2M_1M_2+2M_2-1)\times 1}$ are from $\tilde{\boldsymbol{A}}$ and $\tilde{\boldsymbol{I}}$. $\tilde{\boldsymbol{A}}_1$ is also the dictionary matrix, similar as (16), it can be defined as

$$\tilde{\boldsymbol{A}}_1 = [\boldsymbol{a}_{\tau_1}, \ldots, \boldsymbol{a}_{\tau_i}, \ldots, \boldsymbol{a}_{\tau_Q}] \tag{24}$$

where the mth element of the column vector $\boldsymbol{a}_{\tau_i}$ is $e^{-j2\pi\frac{J_m}{T}\tau_i}$, J_m represents the position index of the virtual pilots, $J_m \in [-M_1M_2 - M_2 + 1, M_1M_2 + M_2 - 1]$.

Based on (23) and utilizing the sparseness of underwater acoustic communication channels, OMP algorithm is adopted in this paper to estimate the path delays $\hat{\tau}_i$ and amplitudes $\hat{\xi}_i$. In OMP algorithm, vector $\boldsymbol{r}$ is correlated with all the columns in the dictionary matrix $\tilde{\boldsymbol{A}}_1$ at each iteration, and the column corresponds to the maximum correlation value identifies the path delay. Then a LS problem is solved to calculate the amplitude corresponding to the path delay. At each iteration, we compare the residual fitting error and the reduction of the fitting error with the threshold based on noise power to determine the termination of the algorithm. After obtaining the estimates of the path delays

and corresponding amplitudes, the channel frequency response can be re-constructed for data decoding.

In summary, the channel estimation scheme proposed in this paper first designs a super-nested pilot structure for OFDM communication systems. Next, in the receiver side, the pilot covariance matrix is modeled. The cross-correlation interference between the signals of each path is estimated by the initial channel estimation to carry out interference cancellation from the covariance matrix. In addition, in order to further approximate the ideal covariance matrix model in the condition of small number of snapshots, SPICE algorithm is used to refine the covariance matrix. Then, according to the pilot position difference, the covariance matrix elements are selected and rearranged as the received signal on continuous and uniform virtual pilot subcarriers. At last, OMP algorithm is utilized to estimate the channel based on the so-called virtual pilot obtained in the previous step. Through these steps, the ultimate goal is to achieve effective estimation of large delay spread channels with limited amount of pilots. The proposed channel estimation scheme is summarized in Algorithm 2.

Algorithm 2 Proposed Channel Estimation Scheme

1: Design super-nested structure pilot distribution
2: In the receiver side, complete pilot compensation to obtain the received signal on the pilot subcarriers $\check{\boldsymbol{z}}$
3: Establish the pilot subcarrier covariance matrix model $\bar{\boldsymbol{R}}_{zz}$ with a small number of snapshots
4: Execute initial channel estimation based on $\check{\boldsymbol{z}}$ to estimate multipath delay $\hat{\tau}_l$ and amplitude $\hat{\xi}_l$
5: Calculate the cross-correlation matrix $\hat{\boldsymbol{R}}_{cor}$ and carry out initial interference cancellation: $\hat{\boldsymbol{R}}_{zz}^{1} = \bar{\boldsymbol{R}}_{zz} - \hat{\boldsymbol{R}}_{cor}$
6: Adopt SPICE algorithm to refine the pilot subcarrier covariance matrix $\hat{\boldsymbol{R}}_{zz}$ based on $\hat{\boldsymbol{R}}_{zz}^{1}$
7: Vectorize the covariance matrix $\hat{\boldsymbol{R}}_{zz}$ from previous step, then screen and rearrange it to obtain virtual pilot position vector $\boldsymbol{r}_1$, which basically consists of dealing with repeated elements and rearranging elements according to the position difference set
8: Execute OMP algorithm for channel estimation based on the received signal $\boldsymbol{r}_1$ on the virtual pilots

3.4. Time-varying channel estimation

In underwater acoustic communication, when the communication distance is far greater than the water depth, the angle of the multipath reaching the receiver is similar, and Doppler effect is dominated by transmitter/receiver relative motion [16]. In this channel setting, a considerable number of literatures have proposed effective solutions to the problem of wideband Doppler estimation and compensation [17–19]. Therefore, we assume that the wideband Doppler effect of the channel has been effectively estimated and compensated, and focus on that there is only residual narrowband Doppler which causes time-varying effect. Targeting at this channel condition, we further propose to use the polynomial estimation method for the time-varying multipath complex gain, based on which the channel matrix with inter-carrier interference is reconstructed [20]. Specifically, the variation of each path's complex gain is approximated by a polynomial within several OFDM symbols. Meanwhile, the multipath delay information is still estimated based on the proposed scheme utilizing observation vector on the virtual pilots.

First, we briefly review the process of estimating the time-varying multipath complex gain based on the polynomial model. Assuming that N_c OFDM symbols are transmitted, and the complex gain of the lth path of the symbols is $\boldsymbol{\alpha}_l$, which can be expressed as

$$\boldsymbol{\alpha}_l = [\alpha_l(-N_g T_s), \alpha_l((-N_g+1)T_s), \dots, \alpha_l((\upsilon N_c - N_g - 1)T_s)] \tag{25}$$

Table 2
Parameters of CP-OFDM.

Bandwidth B	50 kHz
Carrier frequency f_c	250 kHz
Number of subcarriers N	1024
Number of pilots N_p	128
Symbol duration T	20.48 ms
Cyclic-prefix length T_{cp}	19.52 ms
Modulation type	QPSK

Here T_s is the sample interval, N is the sample length of OFDM symbol, N_g is the length of the CP, and $\upsilon = N + N_g$. The duration of an OFDM symbol can be written as υT_s. Using the polynomial model established by N_c coefficients to approximate the complex gain of the path, the following model can be obtained

$$\alpha_l(qT_s) = \sum_{d=0}^{N_c-1} c_{d,l} q^d + \xi_l[q] \tag{26}$$

where $\boldsymbol{c}_l = [c_{0,l}, \dots, c_{N_c-1,l}]^T$ represents N_c polynomial coefficients, $q \in [-N_g, \upsilon N_c - N_g - 1]$, $\xi_l[q]$ represents model error. In another word, the time-varying complex channel gain α_l at any sample time qT_s is approximated by a polynomial with order $N_c - 1$. Polynomial coefficients $\boldsymbol{c}_l$ can be calculated based on the average complex gain $\bar{\boldsymbol{\alpha}}_l = [\bar{\alpha}_{l,0}, \dots, \bar{\alpha}_{l,N_c-1}]$ of the lth path, which means the optimal solution $\boldsymbol{c}_{des_l}$ of $\boldsymbol{c}_l$ is

$$\boldsymbol{c}_{des_l} = \boldsymbol{T}^{-1} \bar{\boldsymbol{\alpha}}_l \tag{27}$$

where $\boldsymbol{T} \in \mathbb{C}^{N_c \times N_c}$ denotes the transformation matrix. [20] shows that $N_c = 2$ can achieve performance very close to the best, so this paper uses $N_c = 2$, and then $\boldsymbol{T} = [1, \frac{N-1}{2}; 1, \frac{N-1}{2} + \upsilon]$.

Based on aforementioned polynomial model, the proposed method to handle time-varying channel introduced by residual narrowband Doppler can be summarized as following steps. First, N_c OFDM symbols are utilized, which have their pilots follow super-nested structure, so as to estimate large delay spread channel. In this paper, $N_c = 2$ is adopted. Second, in the receiver side, based on the observation vector corresponding to the virtual pilots, OMP algorithm is adopted to estimate the delay of the paths, denoted as $\hat{\boldsymbol{\tau}}_{est} = [\tau_1, \tau_2, \dots, \tau_L]$. Next, based on each symbol's own observation vector $\check{\boldsymbol{z}}$ shown in Eq. (6), the average complex gain $\bar{\boldsymbol{\alpha}}_l$ is estimated using the LS method. Denote the set of the average complex gain of L multipaths to be $\bar{\boldsymbol{\alpha}} = [\bar{\boldsymbol{\alpha}}_1, \dots, \bar{\boldsymbol{\alpha}}_L]$, the best polynomial coefficient matrix is then estimated as $\hat{\boldsymbol{C}}_{des} = \boldsymbol{T}^{-1}\bar{\boldsymbol{\alpha}}$, where $\hat{\boldsymbol{C}}_{des} = [\hat{\boldsymbol{c}}_{des_1}, \dots, \hat{\boldsymbol{c}}_{des_L}]$. Finally, the complex gain $\hat{\boldsymbol{\alpha}} = \{\hat{\alpha}_1(qT_s), \dots, \hat{\alpha}_L(qT_s)\}$ is approximated by the polynomial coefficient model, where $\hat{\alpha}_l(qT_s) = \sum_{d=0}^{N_c-1} \hat{c}_{d,l} q^d$ and $\hat{c}_{d,l}$ is the dth element of vector $\hat{\boldsymbol{c}}_{des_l}$. The channel frequency response matrix $\hat{\boldsymbol{H}}$ is then reconstructed by using time delay $\hat{\boldsymbol{\tau}}_{est}$ and complex gain.

4. Simulation results

Simulations in a sparse and large delay spread underwater acoustic communication channel setting are carried out to validate the performance of the proposed channel estimation scheme. The channel has 5 randomly generated paths, with the inter-arrival time of two neighboring paths following an exponential distribution with mean value 4 ms, so the average delay spread of the channel is 16 ms. The amplitudes of paths are Rayleigh distributed, with average power decreasing exponentially with the delay, where the difference between the beginning and the end of the guard time of 19.52 ms is 20 dB. The parameters of the simulated CP-OFDM system are summarized in Table 2. In the simulations, the ratio of the average delay spread to the OFDM symbol duration T is around 0.78, thus it can be considered as an underwater acoustic channel with large delay spread.

In the simulation, 5 snapshots of OFDM symbols are adopted for channel estimation, during which period the channel is assumed to

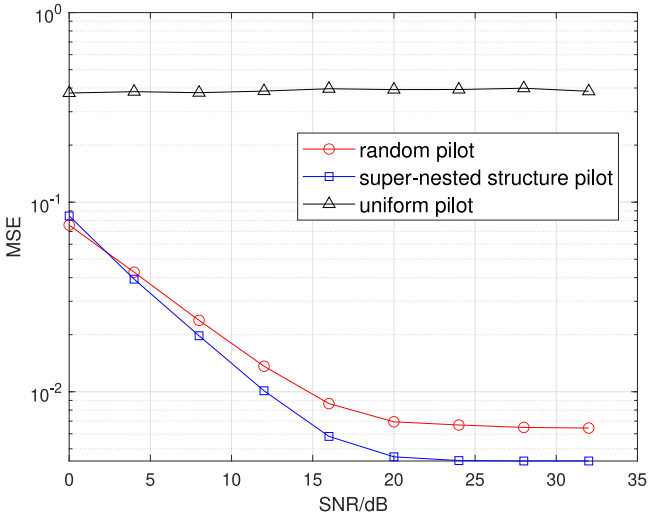

Fig. 1. The comparison of MSE performances with different pilot distributions.

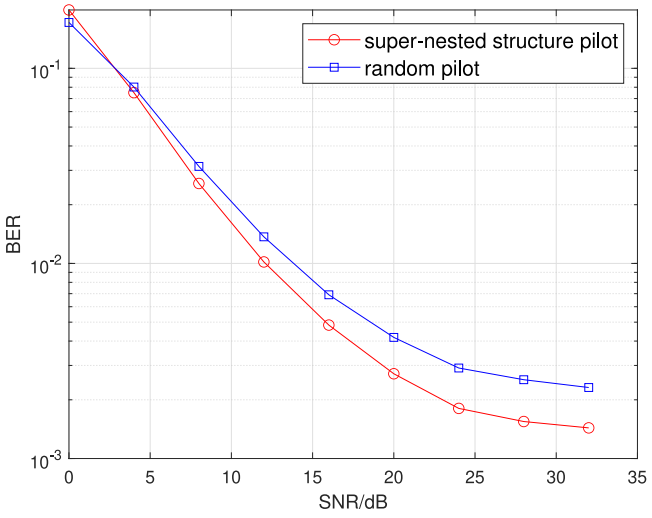

Fig. 2. The comparison of uncoded BER performances.

be stable. For the proposed and reference channel estimation schemes, OMP algorithm with oversampling factor $\lambda = 8$ is adopted. The performance measures are the mean squared error (MSE) of the estimated channel frequency response and bit error rate (BER). The proposed channel estimation scheme based on super-nested pilot structure is compared with direct OMP based channel estimation with random and uniform pilot structures. For all the channel estimation schemes, the number of pilots $N_p = 128$. In super-nested pilot structure, to obtain maximum number of continuous pilot position difference, in this paper, the sizes of the two sub-arrays are $M_1 = M_2 = 64$. The random pilot structure adopted in the simulations is the optimized one which minimizes the maximum cross-correlation between columns of the dictionary matrix [21].

Fig. 1 shows the MSE performances corresponding to different pilot distributions. It is inferred that the ratio of the delay range that can be effectively estimated by the uniform pilot to the symbol duration is 0.125. The uniform pilots' periodicity makes it unable to estimate the large delay spread channel, and its performance is poor. On the contrary, the proposed scheme based on super-nested structure pilot and the direct estimation based on random structure pilot can effectively estimate the large delay spread sparse channel. Comparison of the MSE performances between the proposed super-nested structure pilot scheme and the random structure pilot scheme shows that the proposed scheme can estimate the channel more accurately at most of the signal-to-noise ratio (SNR) range, i.e., when SNR is larger than 3 dB.

Table 3
Complexity comparison of channel estimation schemes.

Channel estimation scheme	Complexity
Proposed scheme	$\mathcal{O}(GN_p^3 + L_1\lambda N_p^2 + L_2\lambda N_v^2)$
Random structure pilot scheme	$\mathcal{O}(L_3\lambda N_p^2)$

Fig. 2 presents the uncoded BER performances of the proposed scheme with super-nested structure pilot and direct estimation with random structure pilot, where similar information can be observed as for the MSE performances. At most of the SNR range, the proposed scheme with super-nested structure pilot can further improve the accuracy of channel estimation and reduce the BER by constructing virtual uniform pilots, which means more virtual pilots than the actual number of pilots are utilized in channel estimation. At BER level of 10^{-2}, around 2 dB gain is obtained by the proposed scheme with super-nested structure pilot than the reference scheme with random pilot.

Next, the computational complexity is analyzed. The complexity of the proposed scheme is mainly composed of three parts: OMP algorithm pre-estimates the channel based on the actual pilot signal, SPICE algorithm refines the covariance matrix, and OMP algorithm re-estimates the channel based on the virtual pilots. The complexity of the SPICE algorithm is mainly determined by the inverse operation of the covariance matrix $\hat{\boldsymbol{R}}_{zz}^{g}$ in each iteration. The dimension of $\hat{\boldsymbol{R}}_{zz}^{g}$ is $N_p \times N_p$, after G iterations, the complexity is $\mathcal{O}(GN_p^3)$. The complexity of the OMP algorithm mainly depends on the estimation of the path delay, that is, the calculation of the inner product function based on the dictionary matrix. It is assumed that the method proposed in this section first pre-estimates L_1 paths based on N_p pilots using OMP algorithm, and the complexity of inner product operation is $\mathcal{O}(L_1\lambda N_p^2)$. Then, based on virtual pilots, OMP is used to estimate L_2 paths. The number of virtual pilots is $N_v = 2M_1M_2+2M_2-1$, and the complexity of inner product operation is $\mathcal{O}(L_2\lambda N_v^2)$. Similarly, it is assumed that the random pilot distribution scheme uses OMP to estimate L_3 multipaths, and the complexity of the inner product operation is $\mathcal{O}(L_3\lambda N_p^2)$. The complexity comparison results are shown in Table 3. In general, the proposed method uses more complexity to achieve better performance.

In addition, for the estimation of time-varying large delay spread sparse channels, the performance of super-nested structure pilot, random pilot, and systematic pilot is compared. For all the pilot structures, polynomial estimation method is adopted to obtain time-varying multipath complex gain, as described in Section 3.4, and $N_c = 2$ OFDM symbols are utilized. For the systematic distribution pilot design, it has the following characteristics: first, the uniform pilot is set at an equal interval of 16, and then two pilots are placed adjacent to the original uniform pilot at an interval of 32. Therefore, the distribution characteristic of three consecutive pilots as a cluster is presented. For all the 3 schemes, the pilot number of each OFDM symbol is $N_p = 128$. The residual Doppler frequency shift adopted in the simulation is $f_d = 0.05/T = 2.44$ Hz, and the multipaths are generated in the same way as the previous setting.

Fig. 3 presents the simulated uncoded BER performances corresponding to the three pilot distributions in time-varying channel. It can be seen that for time-varying large delay spread sparse underwater acoustic channel, the super-nested structure pilot distribution adopting polynomial estimation method still has the best performance. Because of the limited amount of pilots, the systematic pilot design also suffers from the periodic ambiguity generated from uniform clusters, and hence it cannot handle large delay spread channel very well.

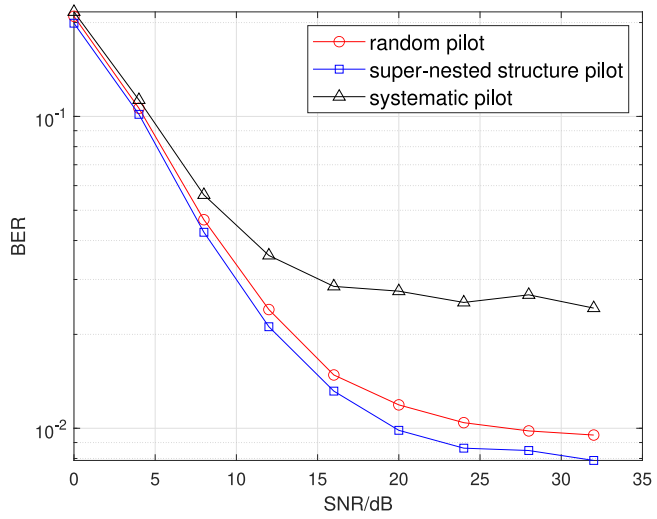

Fig. 3. The comparison of uncoded BER performances of three pilot distribution schemes in time-varying channel.

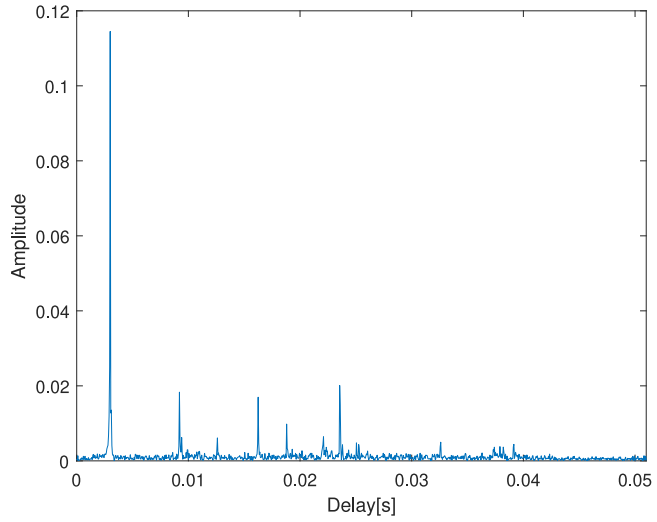

Fig. 4. An example of channel impulse response in the pool experiment.

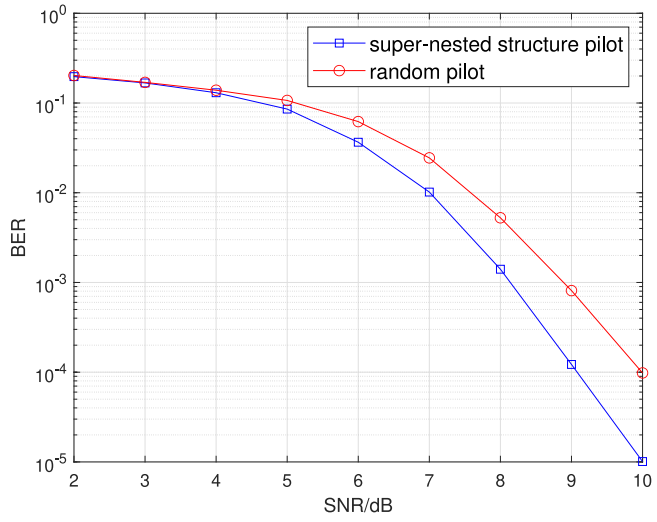

Fig. 5. The comparison of BER performances between the proposed scheme and random structure pilot in pool test.

Table 4
Parameters of CP-OFDM in poor experiment.

Bandwidth B	12.5 kHz
Carrier frequency f_c	250 kHz
Number of subcarriers N	1024
Number of pilots N_p	128
Symbol duration T	81.92 ms
Cyclic-prefix length T_{cp}	80 ms
Modulation type	QPSK

5. Experimental results

5.1. Pool experiment

In order to verify the effectiveness of the proposed channel estimation scheme, a pool experiment was carried out at May 2023, in the Marine Physical Acoustics Laboratory of Xiamen University, Xiamen, Fujian Province, China. The experimental pool is 27 m long, 15 m wide and 2.8 m deep. The distance between the transmitter and the receiver is 8 m, and the water depth is about 1.5 m. The parameters of CP-OFDM system are summarized in Table 4. Besides, 0.5 rate low-density parity-check (LDPC) channel coding was employed. During the experiment, 10 bursts of 5 consecutive OFDM symbols were transmitted and collected.

Fig. 4 shows the channel impulse response of the pool experiment. It can be seen that there are abundant multipath components in the channel, corresponding to the reflection from different walls of the pool. The delay spread of this channel is around 40 ms. The ratio of the delay spread to the symbol duration T is around 0.49, which means the channel can also be considered as large delay spread. Fig. 5 presents the BER performance comparison between our proposed channel estimation scheme and direct channel estimation with random structure pilot in this pool environment. For all the 10 bursts of received OFDM symbols, additional white Gaussian noise is added to generate an average BER curve in the SNR range of 2 dB to 8 dB. It can be observed that the proposed scheme has better estimation performance, and the result coded BER gain increases with the increase of the SNR. At BER level of 10^{-2}, more than 0.5 dB is obtained by the proposed scheme with super-nested structure pilot over direct estimation method with random pilot.

5.2. Sea experiment

A sea trial was carried at May, 2023, at Wuyuan Bay, Xiamen, Fujian Province, China. The distance between the transmitter and receiver was 80 m, and the water depth was about 5 m. The parameter setting of CP-OFDM was the same as shown in Table 2. Quadrature phase shift keying (QPSK) modulation and 0.5 rate LDPC channel coding were employed. During the experiment, 10 bursts of 5 consecutive OFDM symbols were transmitted and collected.

A typical example of channel impulse response in the sea trial is presented in Fig. 6. Compared with the pool experimental channel, the multipath is less in the sea trial, and the delay spread is around 10 ms. The ratio of the delay spread to the symbol duration T is around 0.49. For all the 10 bursts of received OFDM symbols, additional white Gaussian noise is added to generate an average BER curve in the SNR range of 2 dB to 8 dB, which is shown in Fig. 7. It can be observed that the proposed scheme with super-nested structure pilot has better BER performance than direct estimation with random structure pilot, and the gain is more obvious as the SNR grows, from which similar information as shown in Fig. 5 can be observed. At the BER level of 10^{-3}, the proposed scheme obtains about 0.6 dB gain over direct estimation scheme with random structure pilot.

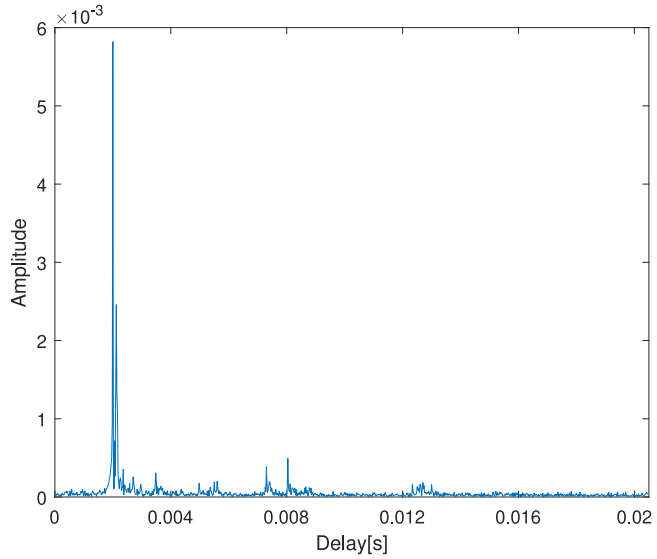

Fig. 6. A typical example of channel impulse response in the sea trial.

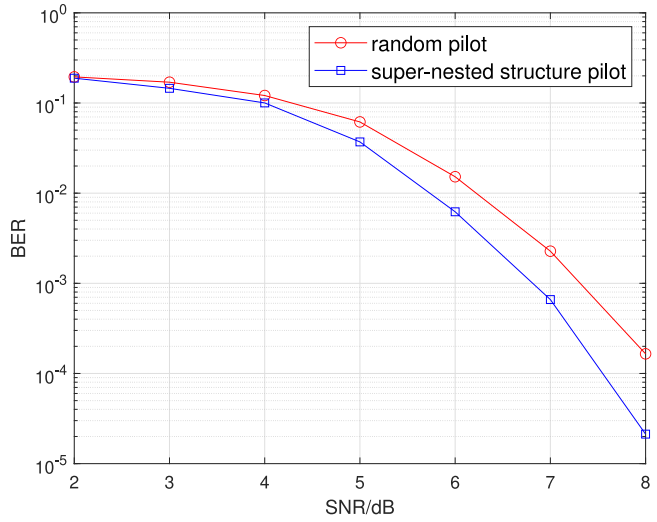

Fig. 7. The comparison of BER performances between the proposed scheme and random structure pilot in sea trial.

6. Conclusion

In this paper, we propose a channel estimation method based on super-nested structure pilot distribution. By constructing virtual continuous uniform pilots, estimation of large delay spread sparse channel can be realized with fewer pilots, which breaks through the limitation of estimation range caused by the periodicity of conventional uniform pilot. Furthermore, initial cross correlation between paths is estimated and canceled out, as well as the SPICE algorithm is utilized to refine the pilot subcarrier covariance matrix. As a result, the accuracy of channel estimation is further improved. Simulation, pool and sea experimental results show that for sparse channels with large delay spread, the proposed channel estimation method can improve the performance when compared with conventional schemes.

CRediT authorship contribution statement

Lei Wan: Writing – original draft, Methodology, Investigation, Funding acquisition, Conceptualization. **Shuimei Deng:** Writing – review & editing, Writing – original draft, Validation, Software, Data curation. **Yougan Chen:** Writing – review & editing, Supervision, Funding acquisition, Formal analysis. **En Cheng:** Resources, Project administration, Funding acquisition.

Declaration of competing interest

The authors declare the following financial interests/personal relationships which may be considered as potential competing interests: Yougan Chen reports financial support was provided by National Natural Science Foundation of China. If there are other authors, they declare that they have no known competing financial interests or personal relationships that could have appeared to influence the work reported in this paper.

Data availability

Data will be made available on request.

Acknowledgments

This work was supported in part by the National Natural Science Foundation of China under Grant 62171394, 62271423, 62271425, U21A20444, and in part by the Sustainable Funding of the Key Laboratory of Underwater Acoustic Technology under Grant JCKYS2022604SSJS001.

References

[1] M. Stojanovic, J. Preisig, Underwater acoustic communication channels: Propagation models and statistical characterization, IEEE Commun. Mag. 47 (1) (2009) 84–89.
[2] M. Stojanovic, Low complexity OFDM detector for underwater channels, in: Proc. IEEE/MTS OCEANS Conf., 2006, pp. 1–6.
[3] B. Li, S. Zhou, M. Stojanovic, L. Freitag, P. Willett, Multicarrier communication over underwater acoustic channels with nonuniform Doppler shifts, IEEE J. Ocean. Eng. 33 (2) (2008) 198–209.
[4] L. Wan, J. Zhu, E. Cheng, Z. Xu, Gridless channel estimation and data detection for underwater acoustic OFDM systems, IEEE J. Ocean. Eng. 47 (4) (2022) 1215–1230.
[5] C.R. Berger, S. Zhou, J.C. Preisig, P. Willett, Sparse channel estimation for multicarrier underwater acoustic communication: From subspace methods to compressed sensing, IEEE Trans. Signal Process. 58 (3) (2010) 1708–1721.
[6] J.A. Tropp, A.C. Gilbert, Signal recovery from random measurements via orthogonal matching pursuit, IEEE Trans. Inf. Theory 53 (12) (2007) 4655–4666.
[7] B. Peng, P.S. Rossi, H. Dong, K. Kansanen, Time-domain oversampled OFDM communication in doubly-selective underwater acoustic channels, IEEE Commun. Lett. 19 (6) (2015) 1081–1084.
[8] E. Panayirci, M.T. Altabbaa, M. Uysal, H.V. Poor, Sparse channel estimation for OFDM-based underwater acoustic systems in Rician fading with a new OMP-MAP algorithm, IEEE Trans. Signal Process. 67 (6) (2019) 1550–1565.
[9] D. Hu, X. Wang, L. He, A new sparse channel estimation and tracking method for time-varying OFDM systems, IEEE Trans. Veh. Technol. 62 (9) (2023) 4648–4653.
[10] M. Oziewicz, On application of MUSIC algorithm to time delay estimation in OFDM channels, IEEE Trans. Broadcast. 51 (2) (2005) 249–255.
[11] S. Qin, Y.D. Zhang, M.G. Amin, Generalized coprime array configurations for direction-of-arrival estimation, IEEE Trans. Signal Process. 63 (6) (2015) 1377–1390.
[12] C.L. Liu, P.P. Vaidyanathan, Super nested arrays: Linear sparse arrays with reduced mutual coupling—Part I: Fundamentals, IEEE Trans. Signal Process. 64 (15) (2016) 3997–4012.
[13] C.L. Liu, P.P. Vaidyanathan, Super nested arrays: Linear sparse arrays with reduced mutual coupling—Part II: High-order extensions, IEEE Trans. Signal Process. 64 (16) (2016) 4203–4217.
[14] P. Pal, P.P. Vaidyanathan, Nested arrays: A novel approach to array processing with enhanced degrees of freedom, IEEE Trans. Signal Process. 58 (8) (2010) 4167–4181.

[15] P. Stoica, P. Babu, J. Li, SPICE: A sparse covariance-based estimation method for array processing, IEEE Trans. Signal Process. 59 (2) (2011) 629–638.
[16] T. Kang, R. Iltis, Iterative carrier frequency offset and channel estimation for underwater acoustic OFDM systems, IEEE J. Sel. Areas Commun. 26 (9) (2008) 1650–1661.
[17] B.S. Sharif, J. Neasham, O.R. Hinton, A.E. Adams, A computationlly efficient Doppler compensation system for underwater acoustic communications, IEEE J. Ocean. Eng. 25 (1) (2000) 52–61.
[18] S. Mason, C.R. Berger, S. Zhou, P. Willett, Detection, synchronization, and Doppler scale estimation with multicarrier waveforms in underwater acoustic communication, IEEE J. Sel. Areas Commun. 26 (9) (2008) 1638–1649.
[19] B. Li, S. Zhou, et al., Multicarrier communication over underwater acoustic channels with nonuniform Doppler shifts, IEEE J. Ocean. Eng. 33 (2) (2009) 198–209.
[20] H. Hijazi, L. Ros, Polynomial estimation of time-varying multipath gains with intercarrier interference mitigation in OFDM systems, IEEE Trans. Veh. Technol. 58 (1) (2009) 140–151.
[21] Q. Jiang, S. Li, H. Bai, R.C. de Lamare, X. He, Gradient-based algorithm for designing sensing matrix considering real mutual coherence for compressed sensing systems, IET Signal Process. 11 (4) (2017) 356–363.